Steel coils versus gas

Gordon P. Blair, Senior Associate Prof. Blair & Associates Northern Ireland & Professor Emeritus, The Queen's University of Belfast, Northern Ireland

discusses Valvetrain Design for MotoGP Engines

This paper was originally published at the Fourth International Conference on "Development Trends of Motorcycles" held in Bologna, Italy in the Ducati Auditorium 10-11 May 2007 and organised by the Haus der Technik (www.hdt-essen.de)

Abstract

In 2002 the FIM (Federation Internationale Motocycliste) sanctioned the use of 990 cm³, naturally aspirated, four-stroke cycle, spark ignition, multi-cylinder engines operating on petrol for racing in the prestige and fastest Grand Prix category, i.e., MotoGP. Most of the engines were of a four-cylinder design and ultimately achieved some 240 hp at about 16000 rpm. For the 2007 season the FIM dropped the engine capacity to 800 cm³, implying that the engines now have a potential target power output of some 200 hp if the peak engine speed is retained at 16,000 rpm. As most of the 990 cm³ engines used coil springs for valvetrain control this implies that the 200 hp target at 16,000 rpm can be achieved using this same valvetrain control system. In the inevitable event that higher power outputs are required to win races and the peak power engine speed rises well above 16,000 rpm then, much as with Formula One car engines when 16,000 rpm was the prevailing engine speed for peak power, it is assumed that pneumatic valve springs will have to be employed. This paper closely examines this contention.

1. The Geometric Layout Design Parameters

On the assumption that a brake mean effective pressure (bmep) of 14 bar can be attained from such engines at peak power where the piston speed is 25 m/s, for a four-cylinder 800 cm³ engine that gives a bore of 74 mm and a stroke of 46.5 mm. A connecting rod length of 95 mm will be assumed, as will an achievable compression ratio of 12.5. This design should then yield the target of 200 hp at 16,100 rpm. The cylinder head design for the top end of this engine is shown in Fig.1 and the intake valve in Fig.2. The outer diameters of the exhaust and intake valves are 27 and 30 mm, respectively [4]. The titanium intake valve shown in Fig.2 has a mass of 14.8 g.

The valve lift diagrams for the intake are created, one rather aggressive with a lift duration-envelope ratio (Kld) of 0.59 labelled as

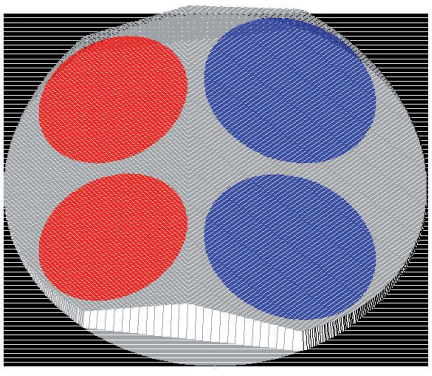

Fig.1 Cylinder head layout.

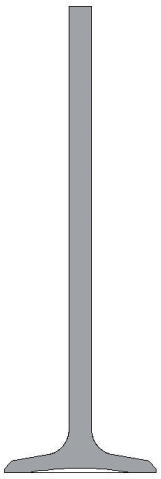

Fig.2 The (titanium) intake valve.

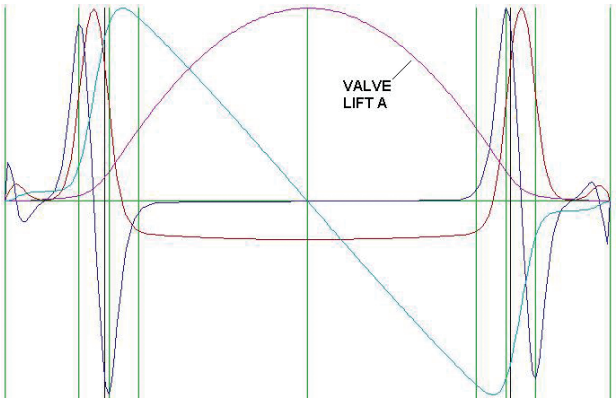

Fig.3 Profile for intake Valve Lift A.

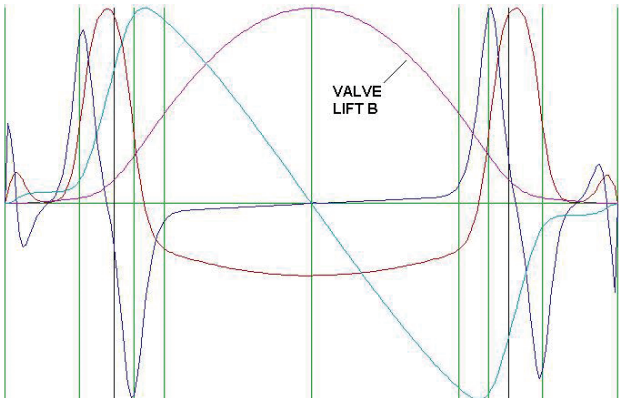

Fig.4 Profile for intake Valve Lift B.

Valve Lift A, and a second somewhat less aggressive lift profile labelled as Valve Lift B with a Kld factor of 0.56 [2, 5, 6]. These are shown in Figs. 3 and 4. The total valve lift for both the intake and exhaust valves is 10.3 mm with the valve lash set at 0.2 mm.

The acceleration diagram for Valve Lift A has a profile quite suitable for a World Championship single-cylinder motocross engine (peak hp at 9000 rpm) whereas that for Valve Lift B could best be described as more typical of a production high-performance multi-cylinder street motorcycle (peak hp at 10,000 rpm). Valve lift profiles with similar aggression levels are created for the exhaust valve [2, 5, 6]. The exhaust (E) and intake (I) opening (O) and closing (C) valve timing events are EO 67 bbdc, EC 45 atdc, IO 52 btdc and IC 72 abdc, where the numbers refer to crankshaft degrees before (b) and after (a) top (t) and bottom (b) dead centre (dc) [1].

Tuned exhaust and intake ducts are designed [1] to accompany the above valvetrain and each are drawn to scale in Figs.5 and 6. The exhaust pipe is a 4-into-1 collector design. The exhaust collector angle shown at 90 degree is simply representational. The profile of the intake bellmouth shown in Fig.6 is optimised [9].

2. The Performance Characteristics

Using the Valve Lift A characteristics, the computed performance characteristics are shown in Fig.7. The power output per cylinder is 37.4 kW or 50.2 hp per cylinder or 201 hp for the entire engine. If the valve lift profiles, Valve Lift B, are employed instead the power output for the 800 cm^3 engine is reduced by some 5 hp at 16,100 rpm. The computation is based on an accurate engine simulation [1] and appropriate and realistic combustion and discharge coefficient maps are employed from that source to accompany the geometric data.

The unsteady gas dynamic behaviour [1] is presented in Figs.8-11 with respect to camshaft angle. In Fig.8 are shown the computed cylinder (CY) and exhaust (EX) and intake (IN) duct pressures, illustrating high quality tuning.

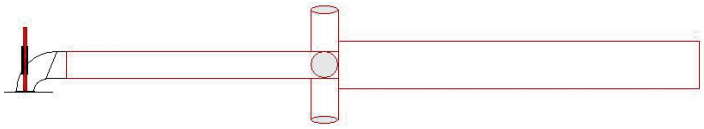

Fig.5 Exhaust system.

In Fig.9 are the dynamic gas particle purity characteristics at the intake valves exhibiting the reverse flows which deteriorate the engine's charging efficiency.

In Fig.10 are the purity characteristics at the exhaust valves illustrating the exhaust and intake pipe tuning that gives a throughflow behaviour during the valve overlap period which enhances the engine's scavenging efficiency and delivery ratio but deteriorates its unburned hydrocarbon emissions.

The Fig.11 is a most important tuning diagram showing the gas particle velocity characteristics close to the intake and exhaust valves in the cylinder head. The fact that the maximum Mach Number is about 0.5 in each case implies that the exhaust and intake pipes have been correctly sized. The reverse flow segments at each end of each diagram coincide with the backflow periods seen in Figs.9 and 10. The bump at about 150 deg (cam angle) on the exhaust particle flow corresponds to the end of the exhaust stroke where the exhaust pipe suction is manfully starting to help scavenge the ever-decreasing cylinder clearance volume.

3. The Mechanical Design Parameters (camshaft)

Quite apart from the dynamic characteristics of the entire valvetrain, the use of either of the two valve lift profiles has major implications for the design of the camshaft and the piston crown. In Fig.12 is shown the valve cut-outs in the piston crown if either Valve Lift A or Valve Lift B is employed. It is quite clear that the more aggressive valve lift profile necessitates deeper, by about 1 mm, valve pockets in the piston ▶

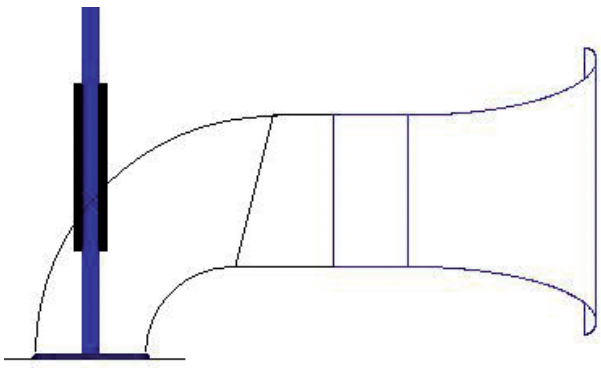

Fig.6 Intake system.

the output data in SI units

power output (kW)	37.42
torque output (Nm)	22.19
delivery ratio	1.233
brake mean effective pressure bmep (bar)	13.95
indicated mean effective pressure imep (bar)	18.9
pumping mean effective pressure pmep (bar)	1.03
friction mean effective pressure fmep (bar)	3.92
brake specific fuel consumption bsfc (g/kWh)	308.7
brake specific CO emissions bsCO (g/kWh)	275.97
brake specific HC emissions bsHC (g/kWh)	10.41
brake specific NOx emissions bsNO (g/kWh)	10.21
charging efficiency	1.191
trapping efficiency	.966
scavenging efficiency	.994
mechanical efficiency	.738
peak cylinder pressure (bar abs)	86.8
peak cylinder temperature (degC)	2239
location of peak pressure (deg atdc)	14.8

Fig.7 The performance at 16100 rpm.

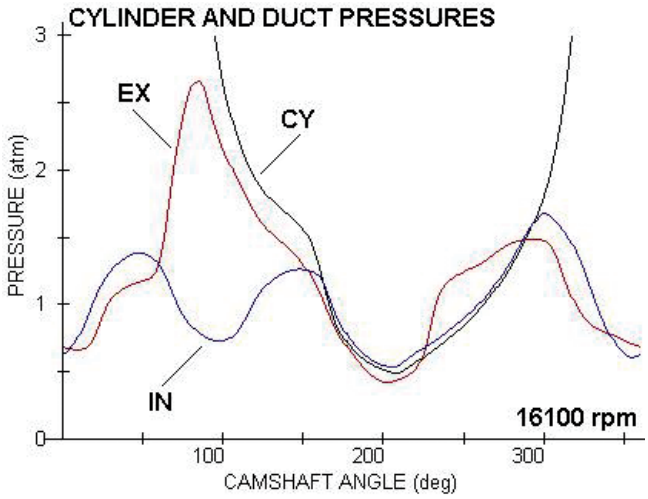

Fig.8 The cylinder and duct pressures.

crown. Good combustion is not aided by deep valve cut-outs in a piston crown.

A finger follower design is used with the valve and camshaft. It has a mass of 15 g and an inertia of 14.82 kg.mm^2. The basic effect of using either valve lift profile is shown in Fig.13. The bulkier cam lobe for Valve Lift A is clearly visible. While the cam to tappet forces will be discussed in greater detail below, it is sufficient at this point to comment that the ensuing maximum Hertz stresses on the cam and tappet interface are just manageable, both being close to 1250 MPa at 16100 rpm.

Of more concern are the oil film characteristics, in this case when a SAE 30 oil at 100 deg C is used as lubricant. These are shown in Fig.14. The oil film thickness profile, with its dip to some 0.35 micron on the opening flank of the cam lobe, is typical of finger followers when a pad is the cam follower. The trough in the oil film thickness profile is due to the reduced entrainment velocity of the oil on the opening flank of the cam. With such a thin oil film, polishing of the cam and cam follower becomes a necessity and hard coating of both a potential solution to scuffing.

The other issue regarding finger follower design is the considerable eccentricity of the valve follower pad on the valve stem giving rise to side forces which causes bending stresses in the valve stem and also higher friction drag in the valve guide. That eccentricity is clearly visible in Fig.13. A potential solution is to use a roller bearing as the valve follower to reduce the side loading on the valve stem but its extra mass at the very end of the finger follower will almost certainly produce an unacceptable increase of inertia for the finger so as to promote valve bounce at high rpm. A better solution is to use a centralised valve follower pad in the form of a scroll, rather than a simple radius, and such a design for the finger follower of Fig.13 is shown in Fig.15.

4. The Mechanical Design Parameters (valvetrain at 16100 rpm)

The valvetrain for the intake valve is analysed dynamically while being motored at 16,100 rpm to ascertain its stability. It should also be analysed under firing conditions [8] but neither time nor space permits such an examination here. It is essential for simulation reality that the dynamic analysis includes, if found to occur, the separation, bounce, and re-attachment of all components. Two types of valve spring design are examined, one with a single coil spring and another with a nitrogen-filled gas spring. The coil spring has 6.5 total coils of 3.75 mm diameter Cr-Si wire with an outer diameter of 25 mm. It has a natural

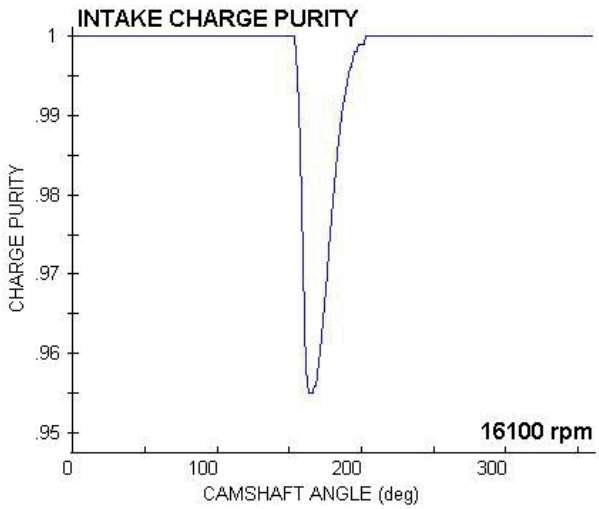

Fig.9 Intake gas purity (air is unity).

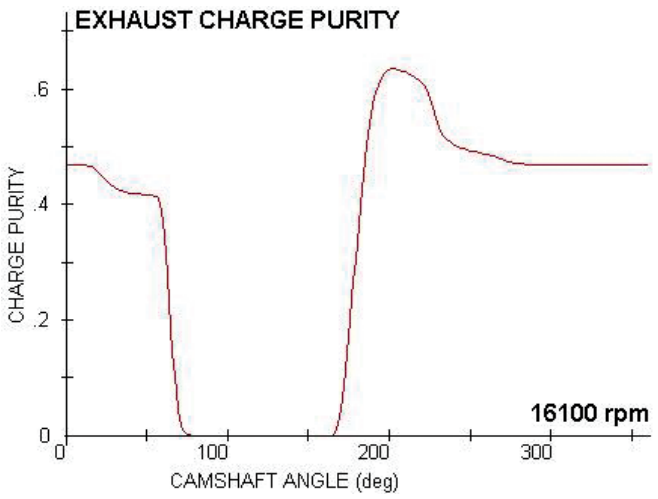

Fig.10 Exhaust gas purity (exhaust is zero).

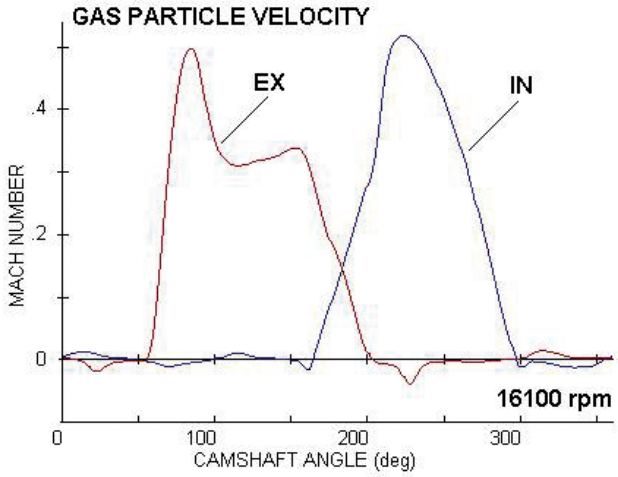

Fig.11 The gas particle velocity characteristics at the exhaust and intake valves.

frequency of 647 Hz, a stiffness of 43.5 N/mm, a preload of 218 N, and a total mass of 35 g. The gas spring has an effective piston diameter of 27 mm and it has a bleed hole of 1.0 mm diameter through which it is fed with nitrogen from a supply rail at a constant pressure of 10 bar.

When the entire coil spring controlled valvetrain is analysed at 16,100 rpm, but using Valve Lift A, the dynamic movement of the valve (DVL) is shown in Figs. 16 and 17 by comparison with the static valve lift (SVL). Valve bounce is observed. This, apparently minor, bounce gives rise to unacceptable levels of acceleration, force, and stress on the head of the valve during bouncing, as seen in Figs.18 and 19.

The acceleration when the valve bounces in Fig.18 is very large, it is actually some 10,000 g, and the forces it engenders at the cam-tappet interface in Fig.19 are also considerable. The source of these problems is to be found in Fig.19, where the aggressive nature of Valve Lift A actually causes the cam follower to loft away from the cam lobe at both opening and closing because the forces are seen to become zero at those locations. The ensuing thump (impulse is the correct word!) when the valve hits the valve seat can be clearly seen in Figs.18 and 19.

The acceleration of the static valve lift, Valve Lift A, is seen to correspond precisely with Fig.3 but the dynamic acceleration (DVL) violently oscillates around it. These unacceptable accelerations and forces on the valve can be contrasted with the effect of using Valve Lift B instead on precisely the same valvetrain geometry. This is shown in Figs. 20 to 22. In Fig.20, there is no valve bounce so there is no

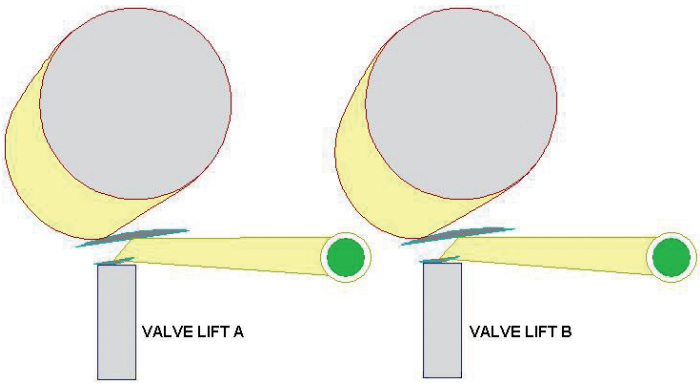

Fig.13 The camshaft and follower design.

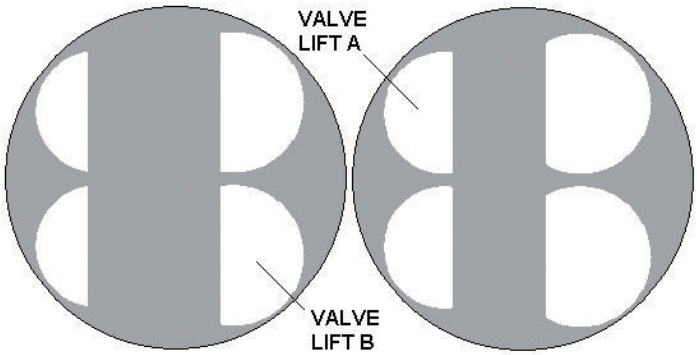

Fig.12 The piston crown pockets.

need to show a similar magnified picture to Fig.17. The maximum acceleration on the head of the valve for Valve Lift B in Fig.21 is a mere 0.016 mm/deg^2, unlike Fig.18 where it rises to over 0.1 mm/deg^2, almost seven times higher.

In Fig.22, the maximum value of the dynamic cam to tappet force for Valve Lift B is 1800 N, whereas it goes nearly 50% higher to 2700 N for Valve Lift A. Observe also that the cam tappet forces never quite reach zero, so there is no separation of cam and cam tappet and, by implication, no tendency for valve lofting.

5. The Mechanical Design Parameters (valvetrain above 16,100 rpm)

If the engine speed is raised above 16,100 rpm, then the higher mass of the spring within a coil spring controlled valvetrain must, at some speed, give rise to instability by comparison with the lighter gas spring. Shown in Figs.23 to 27 are the dynamic valve lifts at 18,000 and 18,500 rpm when the valvetrain is operated with Valve Lift B and with either the coil or the gas spring controlling the valvetrain.

In Fig.23 it can be seen that by 18,000 rpm the valve has lofted under dynamic conditions and is no longer under control, and in Fig.24 by 18,500 rpm it has not only lofted even higher but has bounced several times off the valve seat. This would ultimately result ▶

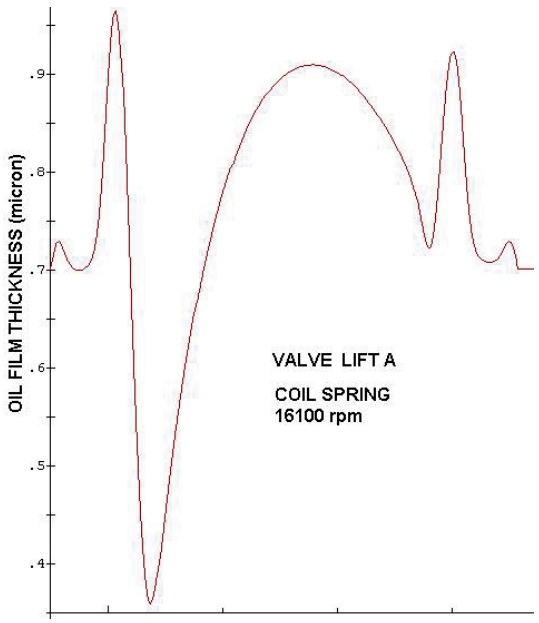

Fig.14 Cam lobe oil film thickness.

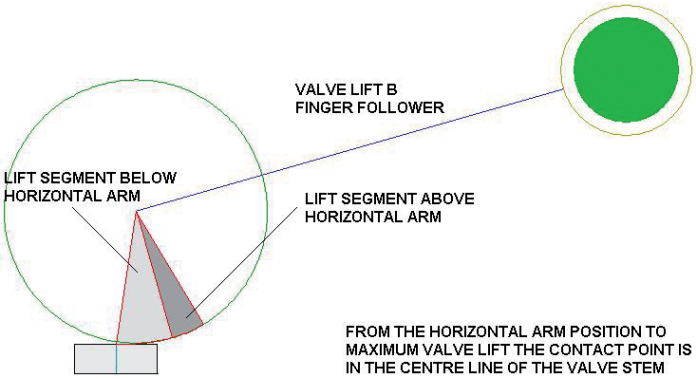

Fig.15 The centralised valve follower tappet.

in breakage of the valve stem/head.

On the other hand, in Figs.25 and 26 it can be seen that the gas spring perfectly controls the valve lift during maximum lift but produces a bounce off the valve seat. Close examination reveals this higher, but softer as it is longer, bounce to have a low stress level for the valve head/stem, by comparison with Fig.23 where there is an apparently similar bounce at 18,000 rpm with the coil spring. A close-up of these valve bounce characteristics is presented in Fig.27.

In Fig.27 it can be seen that the valve bounce with coil spring control changes from marginally unstable at 18,000 rpm to totally unstable by 18,500 rpm. By contrast, the same, or even reduced, soft bounce with the gas spring is repeated at 18,500 rpm. The reasons for this behaviour, when the coil spring controls the identical valvetrain as the gas spring, are encapsulated in Fig.28. This is a snapshot at maximum valve lift of the computed movement of each coil of the coil spring during its stable operation at 16,100 rpm and its unstable behaviour at 18,500 rpm. The left half of each snapshot shows the static movement of each spring coil and in the right half their dynamic movements. The further surge in movement of the upper coils at 18,500 rpm is clearly visible, as is the lofting of the valve, and it is this extra stored energy which propels the valve more rapidly back towards its seat and exacerbates the bounce behaviour. The computed stresses in the lower spring coils also rise dangerously towards 1250 MPa, potentially a fatigue failure level for Cr-Si wire.

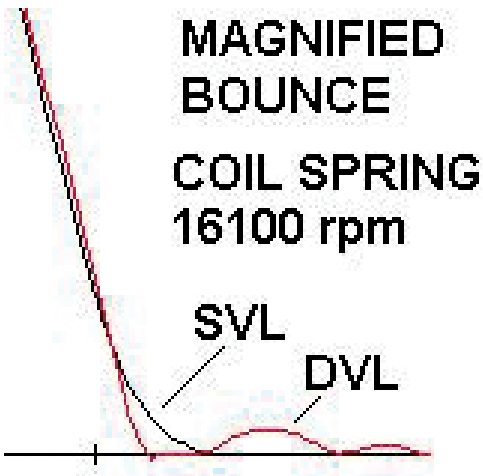

Fig.17 The valve bounce magnified.

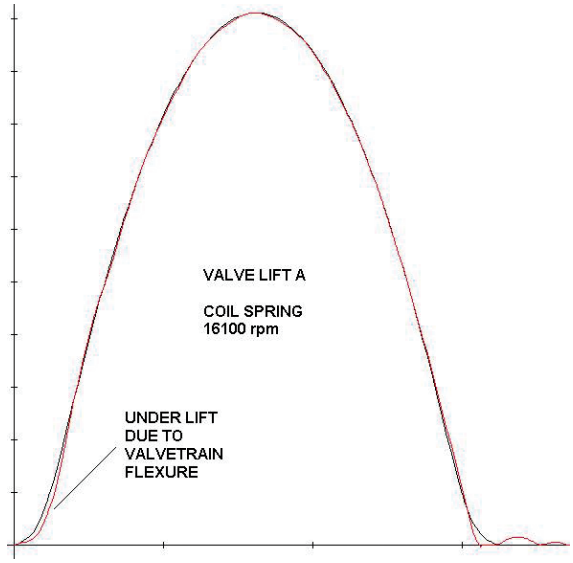

Fig.16 Intake Valve Li ft A at 16100 rpm.

There are several fundamental reasons for the superior valvetrain control by the gas spring at 18,500 rpm. Firstly, the moving piston of the gas spring weighs a mere 8 g by comparison with the 35 g of the coil spring.

Secondly, the use of a bleed hole design for this type of gas spring, it has a diameter of 1.0 mm for the nitrogen gas feed from its 10 bar supply pressure, not only exhibits in Fig.30 a non-linear, i.e., progressive, spring force but also a hysterisis or damping effect as the opening and closing force lines are different. In short, such a gas spring design is a spring-damper system. It will be observed that this produces almost no variance between the static (SVL) forces and the dynamic (DVL) forces.

The internal gas spring pressure behaviour is shown in Fig.29 where its behaviour is plotted over a complete engine cycle of 360 camshaft degrees (720 crankshaft degrees). It will be seen that the pressure at valve opening is some 9.1 bar, which is less than the supply pressure of 10 bar. At valve closing, the pressure has dropped below 9 bar but slowly fills back to 9.1 bar as the valve is about to reopen. To achieve this understanding, the computation must be run for some 40 cycles ▶

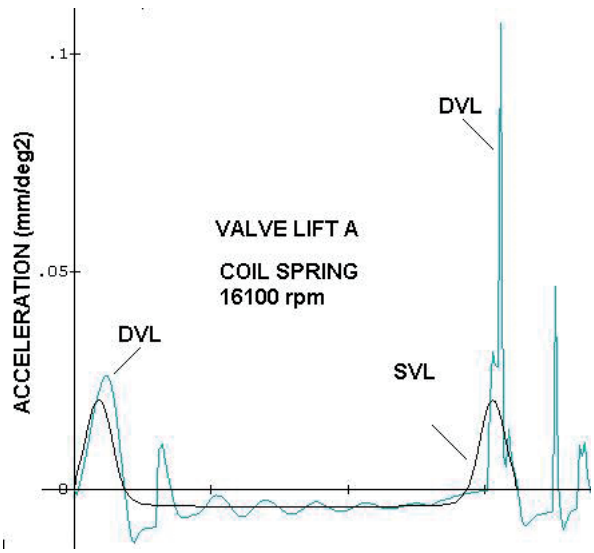

Fig.18 Dynamic valve head acceleration.

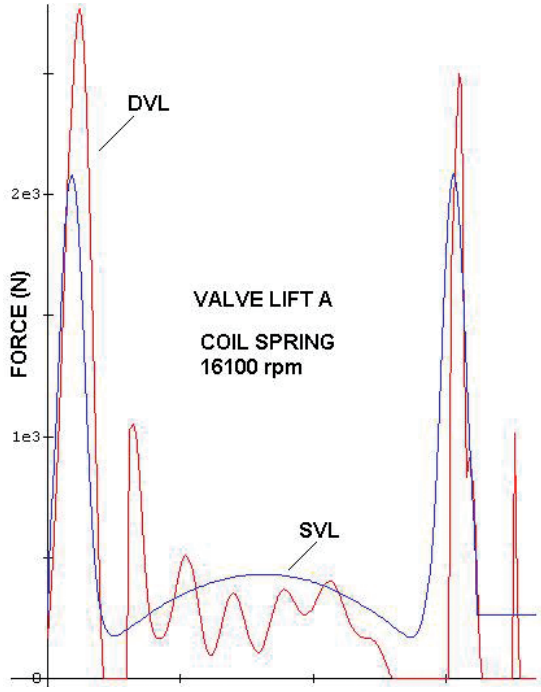

Fig.19 Dynamic cam-tappet forces.

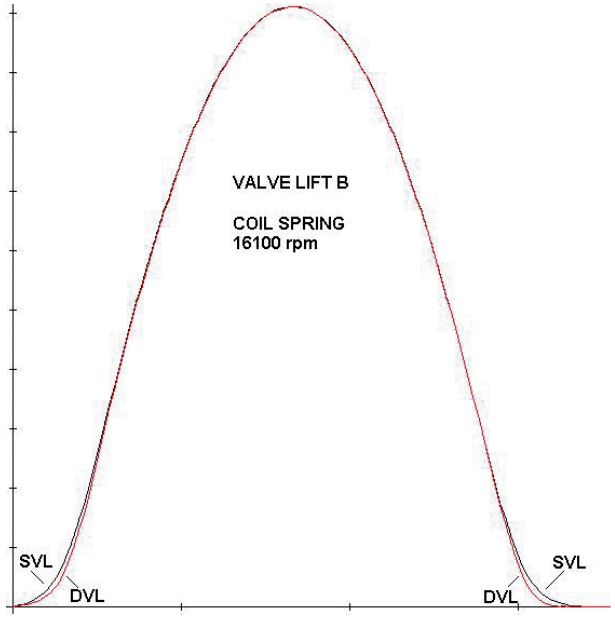

Fig.20 Intake Valve Lift B at 16100 rpm.

of static valve movement to reach equilibrium before beginning the dynamic computation for some 10 further cycles. Needless to add, the unsteady gas dynamic theory to describe this filling and emptying process, into and out of the gas spring, is thoroughly understood and rigorously employed [1].

This apparently odd behaviour is caused by backflow out of the gas spring, through the 1 mm diameter supply hole during valve lift, at higher pressure ratios than is available to refill it before the beginning of the next cycle.

It is this filling and emptying behaviour of the gas spring that provides its damping behaviour and is obviously an important element of the design optimisation process.

Apparently these flow characteristics are less obvious to the writers of some rather expensive software, who persist in predicting gas spring behaviour from the supply pressure and the same PV_ polytropic equations which are taught to freshman undergraduate students everywhere from Belfast to Bologna.

6. Summary

Before 2007, Honda HRC raced a 990 cm^3 V5 engine with a valvetrain which included bucket tappets and a single coil spring per valve. This engine, if paddock rumour is to be believed, produced some 240 hp at 16,000 rpm, reinforcing the conclusion already expressed that 200 hp can be achieved at 16,000 rpm by a four-cylinder 800 cm^3 engine with such a conventional valvetrain. What is also known, perhaps rumoured is again the better word, is that trying to run this same HRC 990 cm^3 engine above 16,000 rpm resulted in some valvetrain problems. Hence, as rumour is always a dangerous commodity, the "contention" expressed in the Abstract did need to be examined as did the "contention" that 200 hp at 16,000 rpm could be theoretically attained.

What is established here is that a valvetrain using coil springs will become unstable at some point in the speed range and that a gas

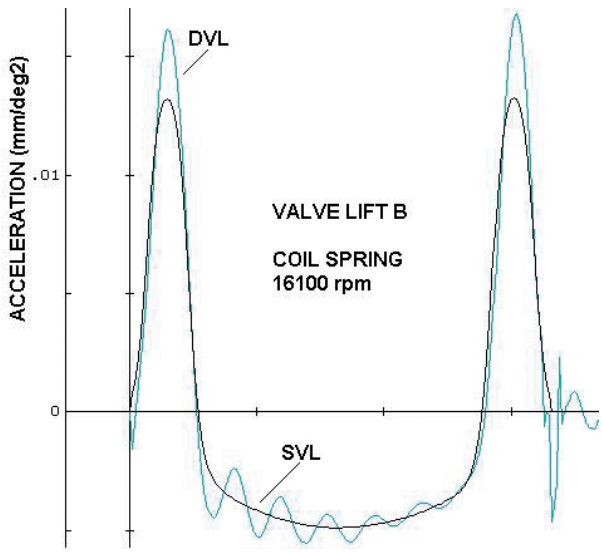

Fig.21 Intake Valve Lift B acceleration.

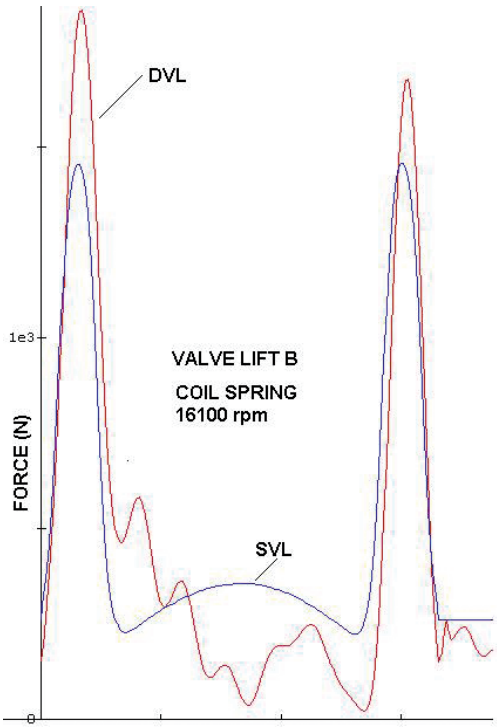

Fig.22 Cam to tappet forces for Intake Valve Lift B.

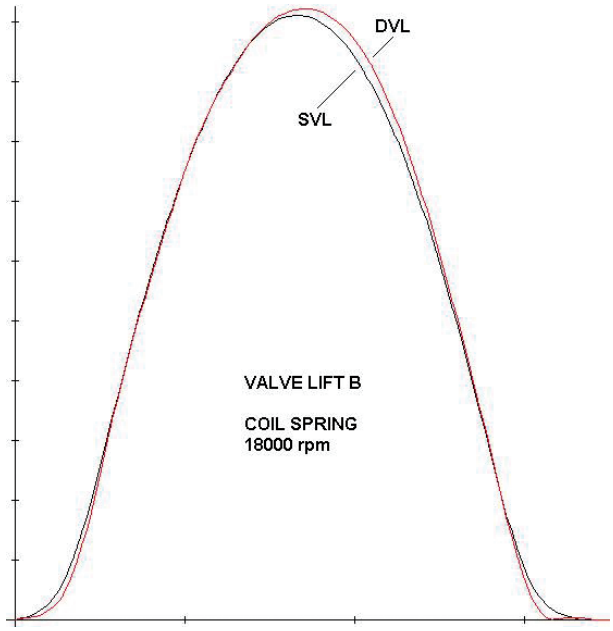

Fig.23 Coil spring at 18000 rpm.

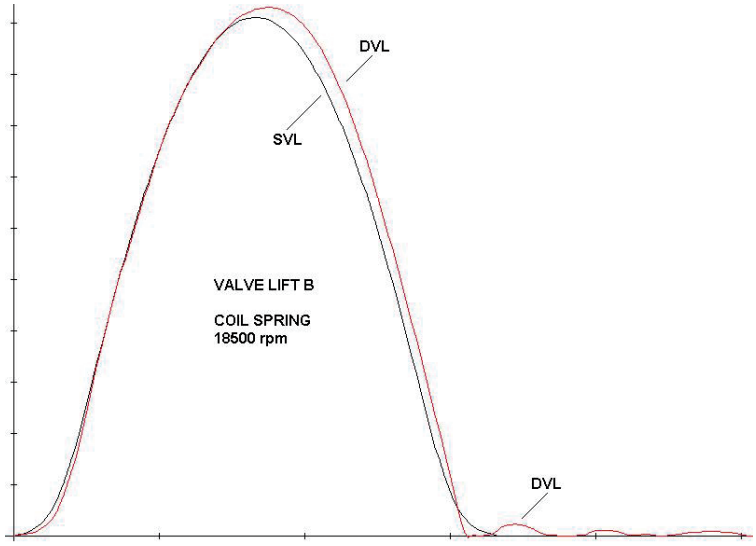

Fig.24 Coil spring at 18500 rpm.

spring control of that same valvetrain will operate to a higher engine speed than with the coil springs, simply because of the reduction in mass being oscillated. All spring systems will ultimately become unstable at some engine speed, but as the gas spring is the lightest spring and most of such designs, but not all, also behave as a spring-damper system, its ability to control the sudden catastrophic bouncing at speeds marginally above stability is considerable (see Fig.27).

Further, it appears from Fig.27 that coil spring control of a finger-follower valvetrain for a 800 cm^3 engine four-cylinder engine could be stable at engine speeds approaching 18,000 rpm. However, it is shown that this is only possible with careful design and selection of the valve lift profile to be employed. Although it has not been examined here, it seems unlikely that the heavier bucket tappet design could be similarly successful as the bucket tappet must weigh at least 25% more than a finger follower and its inertia could well be 30% more at the very least.

The author is very conscious that this paper is being presented in May 2007 in Bologna in the Auditorium of Ducati, who go MotoGP racing with a desmodromic valve control system which essentially contains no valve springs, and that no mention of this unique valve control system has appeared in this paper. While a desmodromic system for valvetrain control theoretically does not permit valve bounce, like all systems it has its own particular design problems. It requires more parasitic power to drive it as the push-and-pull fingers must work to move the valve in both directions, whereas with spring control and no valve lofting the spring returns much of the input work back to the cam and the engine. The return finger of a desmodromic system, being longer and more curved than the lifting finger, is not only a highly stressed but a heavier and/or more flexible component. The reality of the theoretical zero valve bounce will depend on the stiffness, mass and inertia of that component. Having said that, the desmodromic valve control system has been proven by Ducati to be very successful in MotoGP. The author hopes that his hosts will accept these views in the professional spirit in which they are offered and will be most pleased to be corrected, in public, if they are in error. ▶

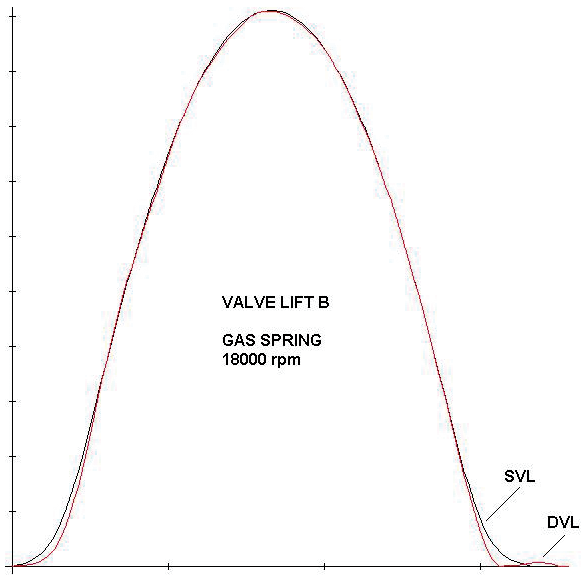

Fig.25 Gas spring at 18000 rpm.

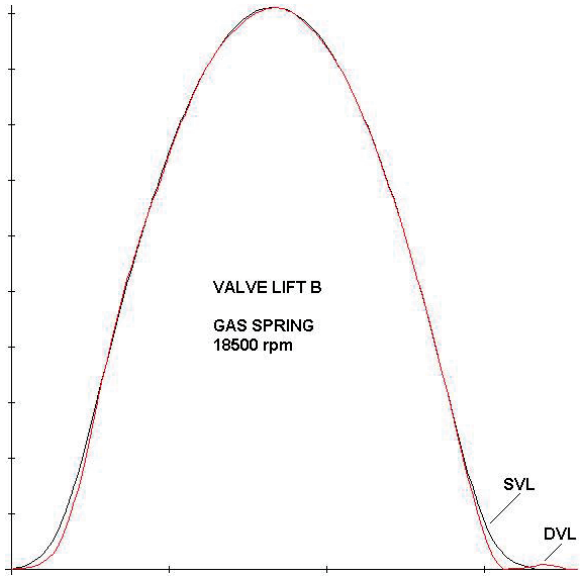

Fig.26 Gas spring at 18500 rpm.

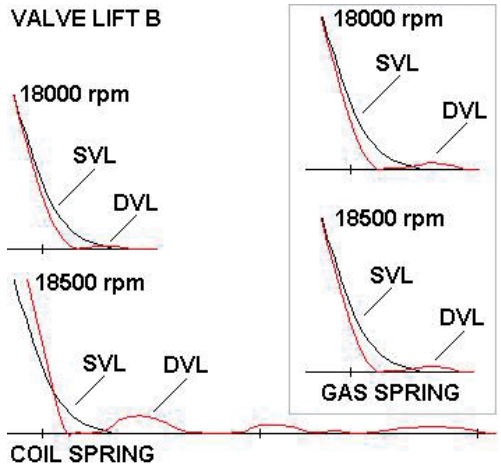

Fig.27 Magnified valve bounce.

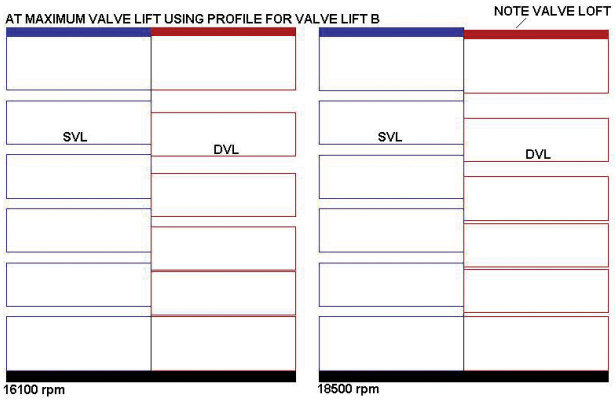

Fig.28 The movement of the coils of the spring.

Acknowledgements

The author would like to thank his fellow Associates [2] for permission to use the 4stHEAD software to execute almost all of the theoretical calculations and which software provides the graphics, which illustrate this paper.

References

1. G. P. Blair, Design and Simulation of Four-Stroke Engines, Society of Automotive Engineers, SAE Reference R-186, 813 pages, 1998.
2. 4stHEAD software suite, Cylinder Head Component Design for Four-Stroke Engines, Prof. Blair and Associates, www.profblairandassociates.com.
3. G. P. Blair, "Die Entwicklungsalternativen für GrandPrixmotorrad-motoren (Design Alternatives for MotoGP Engines)", Entwicklung-stendenzen im Motorradbau, June 2003, Munich, {Haus Der Technik Fachbuch no.28, ISBN-3-8169-2272-4, Essen, www.expertverlag.de}.
4. G. P. Blair, "The Influence of Valve Size Ratio on the Performance of Racing Engines", Conference on "Development Trends for Motorcycles", Bologna, 21-22 April, 2005 {Haus Der Technik Fachbuch no.55, ISBN-3-8169-2549-9, Essen, www.expertverlag.de}.
5. G. P. Blair, C. D. McCartan, H. Hermann, "The Right Lift", Race Engine Technology, Vol. 3 Issue 1, August 2005 (see www.highpowermedia.com and download at www.profblairandassociates.com).
6. G. P. Blair, C. D. McCartan, H. Hermann, "Making the Cam", Race Engine Technology, Vol. 3 Issue 2, October 2005 (see www.highpowermedia.com and download at www.profblairandassociates.com).
7. G. P. Blair, C. D. McCartan, H. Hermann, "Bucket Operation", Race Engine Technology, Vol. 3 Issue 3, December 2005 (see www.highpowermedia.com and download at www.profblairandassociates.com).
8. G. P. Blair, C. D. McCartan, H. Hermann, "Pushrod Operation", Race Engine Technology, Vol. 3 Issue 4, January 2006 (see www.highpowermedia.com and download at www.profblairandassociates.com
9. G. P. Blair, W. M. Cahoon, "Best Bell", Race Engine Technology, Vol. 4 Issue 5, September 2006 (see www.highpowermedia.com and download at www.profblairandassociates.com

Postcript

This paper was originally written for the above-mentioned Conference and presented for publication before the beginning of the 2007 MotoGP season started. Some of its prognostications have already emerged as reality. ■

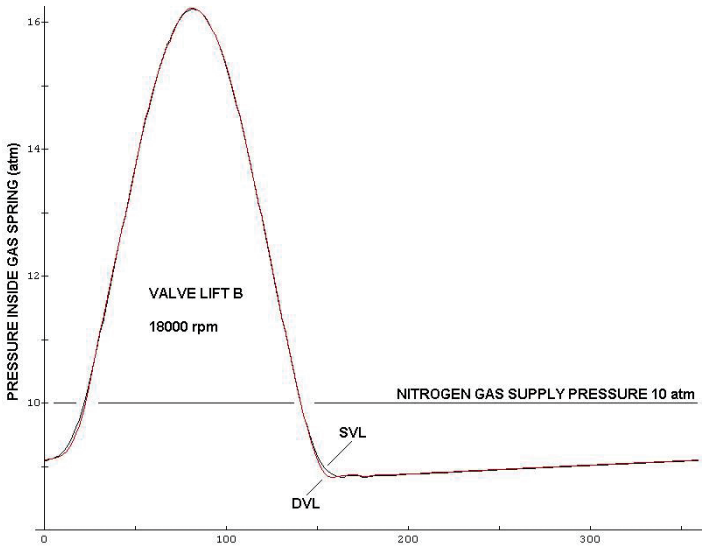

Fig.29 Internal gas spring pressure.

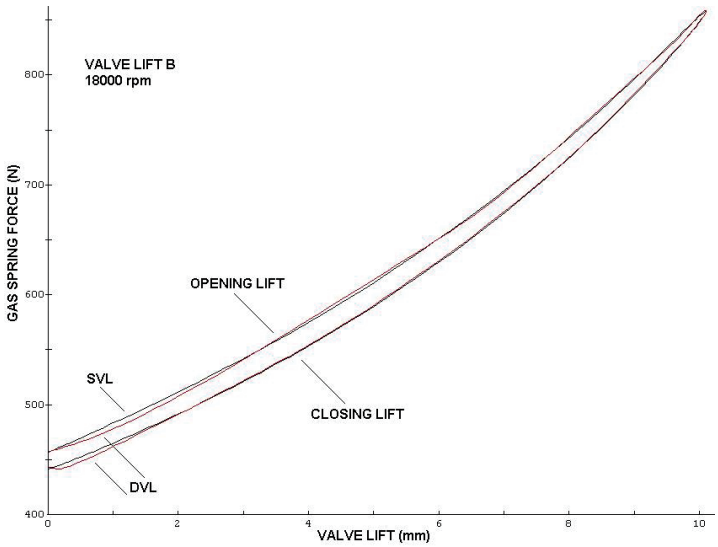

Fig.30 Gas spring force controls valve lift.